Cellular and Molecular Neurobiology (2025) 45:32
https://doi.org/10.1007/s10571-025-01548-y

ORIGINAL RESEARCH

Downregulation of Hmox1 and Rpgrip1l Expression Linked to Risk-Taking Behavior, Reduced Depressive Symptoms, and Diminished Novelty Socialization in SUMO1 Knockout Mice

Qiwei Dai[1] · Yuxiang Wang[2] · Hongbin Xu[3] · He Dong[1] · Fang Nie[1] · Lianxue Zhang[1] · Xiaozhi Liu[2,4,5] · Zhiqing Li[1,3,6]

Received: 20 December 2024 / Accepted: 18 March 2025

Abstract

SUMO1 is involved in the normal physiological functions of the nervous system and is also associated with the development of neurodegenerative diseases. Whereas, the effects and underling mechanisms of SUMO1 knockout (SUMO1- KO) on emotion- and cognition -related behaviors remain unexplored. We investigated changes in depression-like behaviors, social interaction, and cognition in SUMO1-KO mice compared to wild-type (WT) controls using the open-field test, tail suspension test, three-chamber test and novel object recognition test, respectively. To explore the underlying mechanisms of these behavioral differences, we performed Gene Ontology (GO) analysis of proteomics data and subsequently validated the findings through experimental verification. The results showed that SUMO1-KO mice exhibited increased risk-taking behavior, reduced depressive symptoms, and diminished novelty socialization compared to WT mice. Mass spectrometry-based proteomics analysis revealed 370 upregulated proteins and downregulated 84 proteins. GO annotation analysis identified significant enrichment of amino acid transmembrane transporter activities and ion channel. We further investigated two behavior-associated proteins, Hmox1 and Rpgrip1l, and validated their downregulated expression. We concluded that decreased expression of Hmox1 and Rpgrip1l associated with the risk-taking behavior, reduced depressive symptoms, and diminished novelty socialization observed in SUMO1-KO mice.

Graphical Abstract

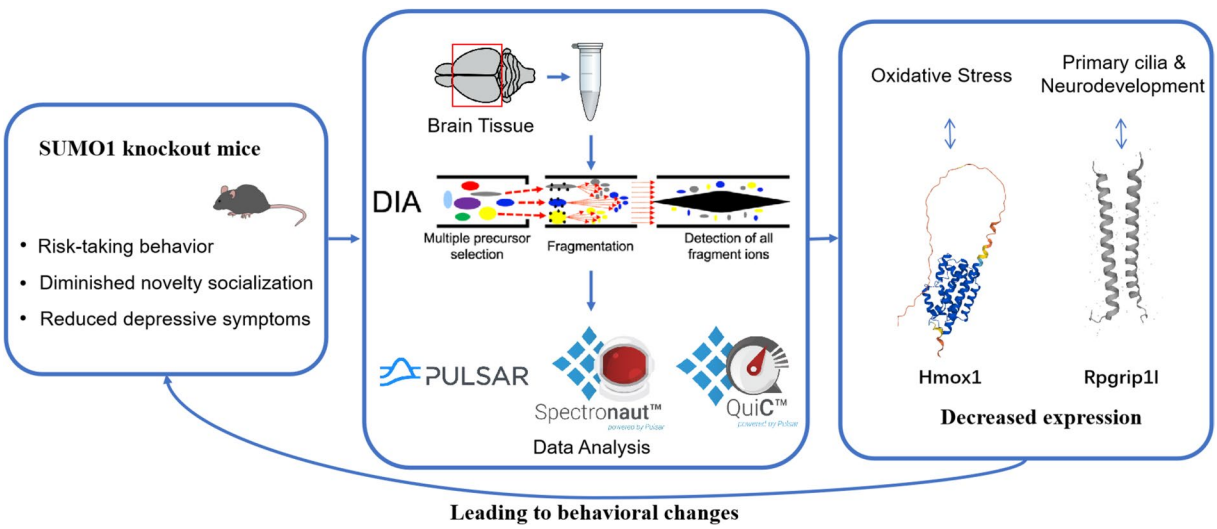

Qiwei Dai and Yuxiang Wang contributed equally to this work and share first authorship.

Extended author information available on the last page of the article

Published online: 01 April 2025

Keywords SUMO1-KO · Exploratory behaviors · Mania-like phenotype · Social interaction · Heme oxygenase 1 · RPGR-interacting protein 1-like

Introduction

Small ubiquitin-like modifier (SUMO) proteins are a family of ubiquitin-like small proteins that covalently attach to target proteins, thereby modulating their function post-translationally. SUMOylation has been shown to conjugate a wide variety of target proteins, regulating many aspects of cell processes, including nucleocytoplasmic transport, transcription, cell-cycle regulation, chromosome segregation, DNA replication, and cell death (Hay 2005; Lomelí and Vázquez 2011; Jackson and Durocher 2013). Prior research has demonstrated the neuroprotective effects of SUMOylation in cerebral ischemic injury (Silveirinha et al. 2013). Furthermore, accumulating evidence suggests that SUMOylation contributes to the pathogenesis of neurodegenerative disease (Krumova and Weishaupt 2013; Lee et al. 2013).

Aging is not simply an accumulation of damage; rather, it is characterized by a significant loss of adaptive genomic information, leading to misallocation and damage across all levels of biological organization, in turn, increases the risk of disease and mortality (Rose 2009). Neurodegenerative disease, such as Alzheimer's disease (AD) and Parkinson's disease (PD), are influenced by several risk factors, with aging been the most prominent (Hou et al. 2019). The regulatory aging processes associated with these diseases include aberrant autophagy, mitochondrial dysfunction, cellular senescence, epigenetic changes, cerebrovascular dysfunction, inflammation, and lipid dysregulation (Gonzales et al. 2022). Major consequence of neurodegenerative disease are cognitive decline and disturbed emotional state (Arioli et al. 2022; Gonzales et al. 2022). Previous studies have demonstrated that compounds such as 1,6-O,O-diacetylbritannilactone and mannan oligosaccharide can attenuate cognitive decline in AD (Liu et al. 2021; Tang et al. 2022).

Mass spectrometry (MS)-based high-throughput proteomics is a pivotal technique for large-scale protein characterization, which is extensively utilized to explore mechanisms underlying neurodevelopment and the pathogenesis of neurodegenerative diseases (Zhang et al. 2014). Using an in vivo chemico-genetic method that employs cell-surface fragment complementation, researchers identified a proteome enriched at astrocyte–neuron junctions through high-resolution liquid chromatography–tandem MS, indicating that neuronal cell adhesion molecule is required to restrict neuropil infiltration by astrocytic processes and providing insights into how astrocytes influence GABAergic synapse formation and functionality (Takano et al. 2020).

Proteomic research by Wenting Xie et al. demonstrated that CEND1 deficiency is linked to mitochondrial dysfunction and cognitive impairment in Alzheimer's disease (Xie et al. 2022). In the human brain samples, AD stage-associated molecular networks were characterized via MS, and comparative analyses of brain tissue and cerebrospinal fluid proteomes highlighted potential biomarker. Coupled with 5xFAD mouse model analyses, Aβ-correlated proteins and AD-related molecules pathways were identified (Bai et al. 2020). Additionally, Ozge Karayel et al. conducted proteomic profiling of cerebrospinal fluid to detect potential biomarkers for PD, identifying proteins such as OMD, CD44, VGF, PRL, and MAN2B1 (Karayel et al. 2022). In ischemic conditions, proteomics identified 112 potential SUMO3 substrates, 91 candidates of which were more abundant in the ischemia group compared to the sham group. Analysis of these proteins highlighted neuroprotective processes, including glucocorticoid receptor signaling, RNA processing, and SUMOylation-dependent ubiquitin conjugation (Yang et al. 2014).

The effects of SUMO1-KO in emotion and cognition -related behaviors have not been fully explored. In this study, we examined anxiety- and depression-like behaviors, social interaction, and cognitive function in SUMO1-KO mice compared to WT mice, employing the open-field test, tail suspension test, three-chamber test, and novel object recognition (NOR) test, respectively. To further elucidate the molecular basis of these behavioral differences, we conducted gene ontology (GO) enrichment analysis on proteomic data and validated key findings from the proteomic analysis.

Materials and Methods

Animals

The SUMO1 knockout ($SUMO1^{-/-}$) mice (Evdokimov et al. 2008) were backcrossed onto C57BL/6 wild-type (WT) background. $SUMO1^{-/-}$ mice were generated by intercrossing heterozygous mice. The primers used for genotyping are as follows:

SUMO1-XA-F1: TCCACCTGCCTCTACCTCAAGTGCTG
SUMO1-XA-F2: GGCTGGCTTAACTATGCGGCATCAGAG

SUMO1-XA-R1: CGCCTAAGTCCTCAGTTGAAGGTTTTGC

The WT and SUMO1$^{-/-}$ male mice (12–18 months old, $n=9$) were used for experiments. The mice were kept in the SPF-grade animal room on the 19th floor of the Experimental Building of Tianjin International Joint Academy of Biotechnology and Medicine. The animal room had a 12-h light–dark cycle, with a relative humidity of 50%, a temperature of 24 °C, and free access to water and food. Mice were housed 2–3 per cage, and were allowed to adapt to the environment for one week before the experiment started. The use and handling of experimental animals for research complied with the requirements of the Animal Ethics Committee of Tianjin Fifth Central Hospital (Approval Number: TJFCH2023043) regarding experimental animal handling and animal welfare.

Chemicals

Retinitis pigmentosa GTPase regulator-interacting protein-1 like (Rpgrip1l) Antibody (No.29778-1-AP; RRID: AB_2923607) was purchased from Proteintech Group Inc (Rosemont, IL, USA), Heme oxygenase 1 (Hmox1) (No. ab68477; RRID: AB_11156457) was purchased from Abcam Inc (Cambridge, UK), β-Tubulin (No.2128S; RRID: AB_823664) and Anti-rabbit IgG, HRP-linked Antibody (No.7074S; RRID: AB_2099233) were purchased from Cell Signaling Technology Inc. (Danvers, MA, USA). Western Bright™ ECL (R-03031-D25) was purchased from advansta Inc. (San Jose, CA, USA). BCA Protein Quantification Kit (PC0020) was obtained from Solarbio (Beijing, China).

Open-Field Test

The open-field test was designed to assess exploratory activity and anxiety-like behavior in mice ($n=9$ for each group). During the test, each mouse was allowed to explore the an open-filed box for ten min. For the Open field test, a camera positioned above the test arena recorded the session. The video was connected to analysis software (Noldus EthoVision Zhenghua, Anhui Province EthoVision 1.19) that automatically recorded and analyzed mouse behavior in the open field. Each mouse was initially placed in a corner of the field, facing the center.

Tail Suspension Test

The tail suspension test was performed to evaluate depression-like behavior in mice ($n=9$ for each group). Each mouse was suspended over a four min period by adhesive tape, attached nearly one cm from the tip of the tail, with the mouse positioned 50 cm above the floor. To record the session, a camera was positioned in front of test arena. Considering the behavioral characteristics of mice in the tail suspension test, to ensure the more accurate assessment, the video was manually evaluated. A mouse, when suspended by the tail for a short period, exhibits alternating periods of agitation and immobility, referred to as the searching and waiting phases, respectively. The searching phase is characterized by body jerks, running motions, and body torsions as the mouse attempts to catch its tail. In contrast, the waiting phase is marked by the absence of initiated movements and includes passive swaying (immobility) (Iyer et al. 2019). The immobility rate was calculated as the duration of the waiting phase divided by the total test duration, with used as an indicator of depressive-like behavior in the mice.

Three-Chamber Test

The three-chamber test was designed to assess social interaction and preference for social novelty in mice ($n=9$ for each group). Mice were initially placed in the center chamber of a three-chamber apparatus, with two empty cages located in the left and right chambers. During the ten min adaptation period, mice were allowed to explore only the center chamber, with the doors to the side chambers closed. In the first test phase assessing social interaction, the doors were opened, and the first stranger of the same age and sex was placed in one of the side cages. The test mouse was then free to explore all three chambers for ten minutes. For the final phase assessing social novelty, the second stranger of the same age and sex was placed in the opposite side cage, and the test mouse was again allowed to explore all three chambers for an additional ten minutes. One camera placed above the test arena captured the session, with the footage processed using Noldus EthoVision Zhenghua, Anhui Province EthoVision 1.19 software, which automatically tracked and analyzed mouse behavior during the three-chamber test.

Novel Object Recognition (NOR) Test

The NOR test was conducted to assess short-term memory retention in mice ($n=9$ for each group). During the adaptation phase, each mouse was allowed to explore two identical objects in the open-filed box for five min. After a 20-min rest period, the testing phase began, in which one of the identical objects was replaced by a novel object of a different size and shape. Mice were then given five minutes to explore the objects, allowing for the assessment of their recognition and memory by measuring their preference for the novel object. To record the session, a camera was positioned above the test arena. Considering the behavioral characteristics of mice in the NOR test, to ensure the more accurate assessment, the video was manually evaluated. Exploration was characterized by the

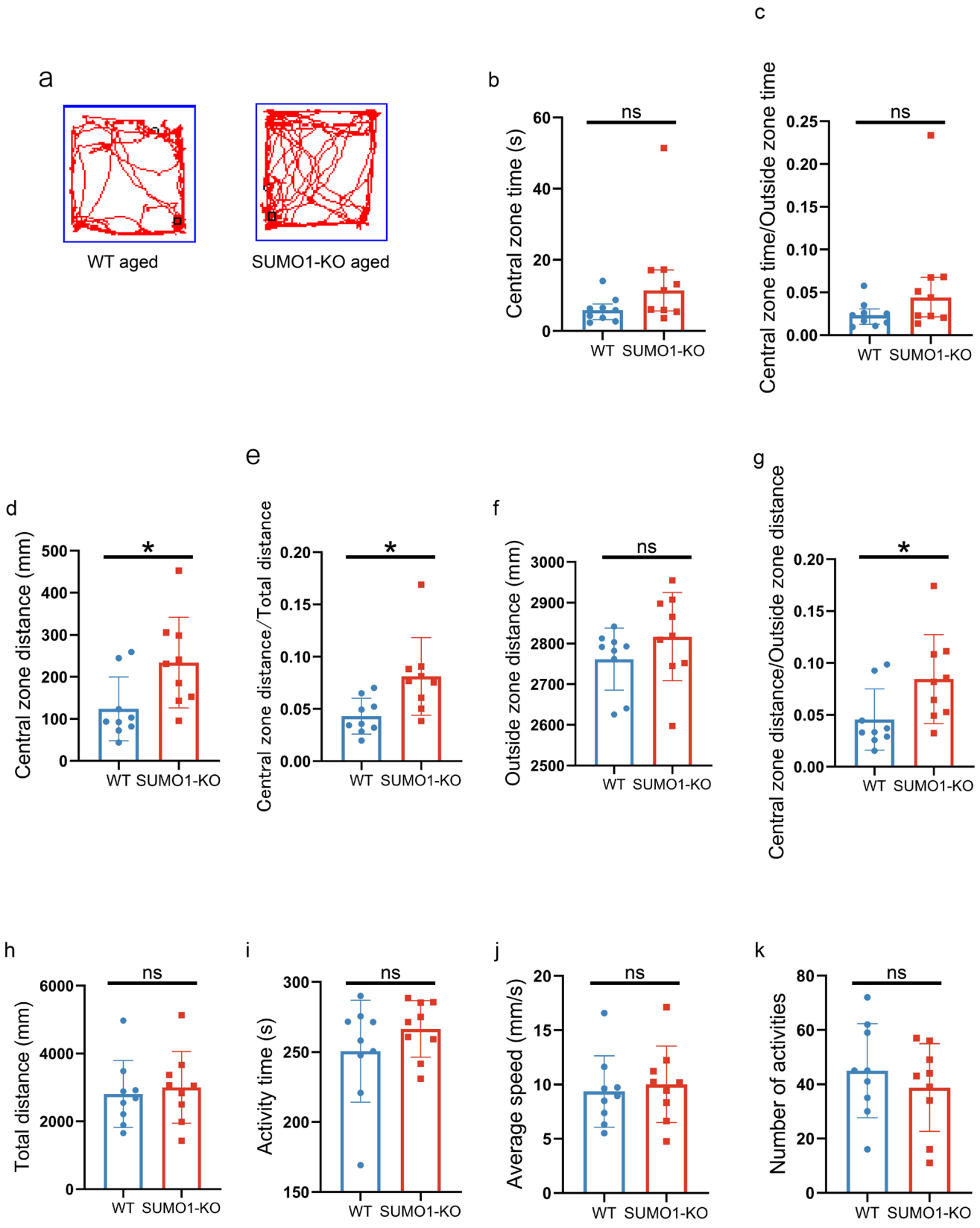
a
WT aged
SUMO1-KO aged
b
Central zone time (s)
ns
WT SUMO1-KO
c
Central zone time/Outside zone time
ns
WT SUMO1-KO
d
Central zone distance (mm)
*
WT SUMO1-KO
e
Central zone distance/Total distance
*
WT SUMO1-KO
f
Outside zone distance (mm)
ns
WT SUMO1-KO
g
Central zone distance/Outside zone distance
*
WT SUMO1-KO
h
Total distance (mm)
ns
WT SUMO1-KO
i
Activity time (s)
ns
WT SUMO1-KO
j
Average speed (mm/s)
ns
WT SUMO1-KO
k
Number of activities
ns
WT SUMO1-KO

◂**Fig. 1** SUMO1-KO mice exhibit an increased tendency for exploration and risk-taking behavior compared to WT controls. **a** Representative movement chart (red trails) in the different groups. Central zone time (**b**) and central zone time/outside zone time (**c**) in the two groups. Central zone distance (**d**), central zone distance/total distance (**e**), outside zone distance (**f**), central zone distance/outside zone distance (**g**) in the two groups. Total distance (**h**), activity time (**i**), average speed (**j**), and number of activities (**k**) in the two groups. Data for **b** and **c** were represented as median and interquartile range, and the other data were represented as mean ± SD. $^{*}p < 0.05$ versus the WT group. $n = 9$ for each group

mouse being in close proximity to an object, orienting its nose toward the object, and displaying active exploratory behaviors such as sniffing. The time spent exploring each object during the NOR test was subsequently used to calculate the discrimination ratio, which is an indicator of its preference for the novel object. The general formula of discrimination ratio is (time spent at novel object − time spent at familiar object)/(time spent at novel object + time spent at familiar object) (Sawangjit et al. 2018).

Proteomics

After the above behavioral experiment, the one side of cerebral hemisphere for each mouse ($n = 5$ for each group) was suspended in lysis buffer containing protease inhibitor. The mixtures were vortexed thoroughly and homogenized three times using a high-throughput tissue grinder. Subsequently, the mixtures were incubated at 4 °C for 30 min, with vortexing every 10 min. After centrifugation, the protein sample were then prepared through a series of steps including denaturation, reduction, alkylation, tryptic digestion, and peptide cleanup. The resulting peptide mixtures were re-dissolved in the buffer A (H_2O, adjusted to pH 10.0 with ammonium hydroxide) subjected to high pH fractionation using a nanoACQUITY UPLC system connected to a reverse-phase column. For nano-HPLC-MS/MS Analysis, peptides were separated with the UltiMate 3000 liquid chromatography system coupled to the timsTOF Pro2 Mass spectrometer. Finally, the DIA raw data were processed and analyzed using Spectronaut 18 (Biognosys AG, Switzerland) with default settings.

To identify proteins with significant expression differences between groups, the threshold for differential expression was set as an absolute fold change (FC) > 1.2 and p-value < 0.05. The FC for each protein was calculated as the mean expression level in the SUMO1-KO group divided by the mean expression level in the WT group. The p-value was determined using Student's t-test, comparing protein abundance between individual samples within the SUMO1-KO and WT groups. Based on the identified differentially expressed proteins, Gene Ontology (GO) annotation enrichment analysis was performed.

Western Blotting

Another side of cerebral hemisphere for each mouse ($n = 5$ for each group) was homogenized and sonicated in cold PBS. Proteins were then extracted in lysis buffer with protease inhibitor. The protein samples were electrophoretically separated onto 10% PAGE gel and then transferred to the PVDF membrane. Membranes were blocked with 5% skimmed milk for 1.5 h, followed by overnight incubation at 4 °C with primary antibodies: Hmox1 (1:1000), Rpgrip1l (1:1000), and β-tubulin (1:1000). The membranes were then incubated with secondary antibody, Anti-rabbit IgG (1:2000), at room temperature for 1 h. Protein detection was performed using an enhanced chemiluminescence system (Tannon, Shanghai, China). The density of each immunoreactive band was measured with Image J software and then normalized to β-tubulin. The specificity of all primary antibodies used has been authenticated by the initial manufacturer, and the information about validation of the primary antibodies are listed in Supplementary Material 1.

Statistical Analysis

Before conducting comparisons among groups, a Normality and Lognormality Test (Anderson–Darling test, D'Agostino&Pearson test, Shapiro–Wilk test or Kolmogorov–Smirnov test) was performed to select the appropriate parametric or non-parametric tests. Furthermore, F test was carried out for variance homogeneity assessment. For data adhering to normal distribution (Parametric data), comparisons between two groups were analyzed with unpaired student t-test (variance homogeneity) or unpaired student t-test with Welch's correction (variance homogeneity was not met). For non-normally distributed data (non-parametric data), comparisons between two groups were analyzed using Mann Whitney test. Parametric data has been presented as mean ± SD, and nonparametric data has been displayed as median and interquartile range. Differences between the two groups were assessed with GraphPad prism 8.0 (GraphPad, San Diego, CA, USA). Statistical significance was set at $p < 0.05$. The results of all statistical tests were represented in the Supplementary Material 2. The sample size for the experimental design was established based on previous publications. This study acknowledged certain limitations, including the omission of a priori sample size calculation, and lack of experimenter blinding.

Results

SUMO1-KO Mice Exhibit an Increased Tendency for Exploration and Risk-Taking Behavior Compared to WT Controls

To assess the effects of SUMO1-KO on exploration and risk-taking behavior, the open-field test was designed. The representative movement chart in different groups were shown in Fig. 1a. The central zone distance ($p = 0.0236$, Fig. 1d), central zone distance/total distance ($p = 0.017$, Fig. 1e), and central zone distance/outside zone distance ($p = 0.0393$, Fig. 1g) in SUMO1-KO group were significantly higher than that in WT group, while the outside zone distance ($p > 0.05$, Fig. 1f) in SUMO1-KO group were slightly higher than that in WT group. However, no significant effects were observed for central zone time ($p > 0.05$, Fig. 1b) or central zone time/outside zone time ($p > 0.05$, Fig. 1c). Similarly, no significant effects were observed for total distance ($p > 0.05$, Fig. 1h), activities time ($p > 0.05$, Fig. 1i), average speed ($p > 0.05$, Fig. 1j) or number of activities ($p > 0.05$, Fig. 1k).

SUMO1-KO Mice Displayed Reduced Depressive-Like Behavior Compared to WT Controls

To evaluate the effects of SUMO1-KO on depression-like behavior, the tail suspension test was performed. Schematic drawing of the tail suspension test was shown in Fig. 2a. The results showed that immobility rate in SUMO1-KO group was significantly lower than that in WT group ($p = 0.0427$, Fig. 2b), implying lower depressive states in SUMO1-KO mice.

SUMO1-KO Mice Exhibit Diminished Novelty Socialization Compared to WT Controls

The three-chamber test was designed to assess the effects of SUMO1-KO on social interaction and preference for social novelty. Schematic drawing of the three-chamber test was shown in Fig. 3a. In sociability test of the three-chamber test, no significant effects were observed for duration with the stranger I compared to the empty side both in WT group ($p > 0.05$, Fig. 3b) and SUMO1-KO ($p > 0.05$, Fig. 3c). In novel sociability test, WT mice exhibited significantly longer duration with the stranger II compared to the strangers I ($p < 0.0001$, Fig. 3e), while SUMO1-KO mice spent slightly shorter time with the stranger II compared to the strangers I ($p > 0.05$, Fig. 3f).

SUMO1-KO Mice Displayed Comparable Memory and Cognitive Abilities Compared to WT Controls

The NOR test was conducted to assess the effects of SUMO1-KO on short-term memory retention. Schematic drawing of NOR test was shown in Fig. 4a. There were no significant differences in discrimination rate between SUMO1-KO and WT group ($p = 0.6783$, Fig. 4b).

Proteomic Analysis of the Impact of SUMO1-KO on Protein Expression

To explore mechanisms underlying the above behavioral effects in the SUMO1-KO mice, MS-based high-throughput proteomics was performed for large-scale protein characterization.

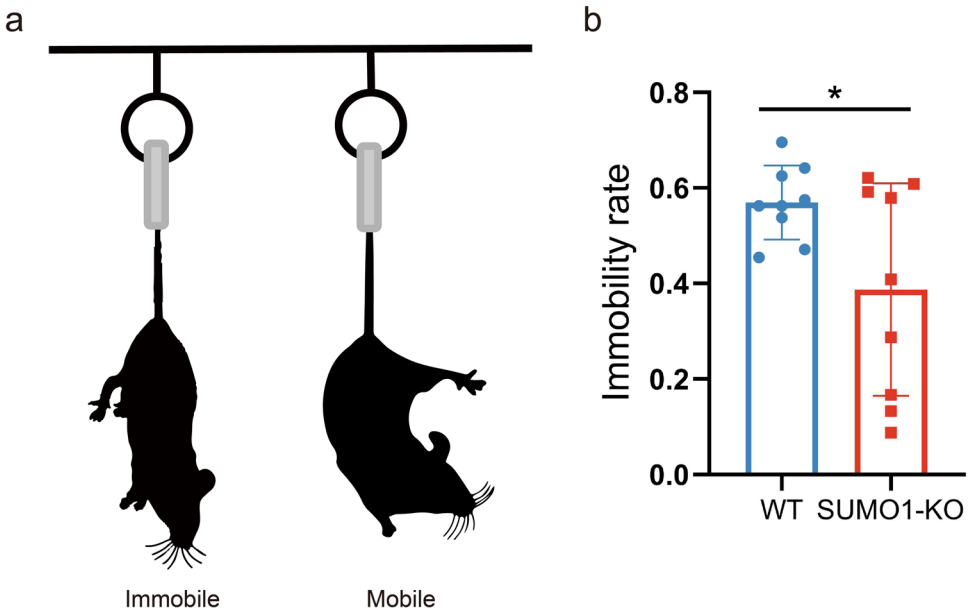

Fig. 2 SUMO1-KO mice displayed reduced depressive-like behavior compared to WT controls. **a** Schematic drawing of the tail suspension test. Created with adobe illustrator. **b** The immobility rate in the two groups. Data were represented as mean ± SD. *$p < 0.05$ versus the WT group. $n = 9$ for each group

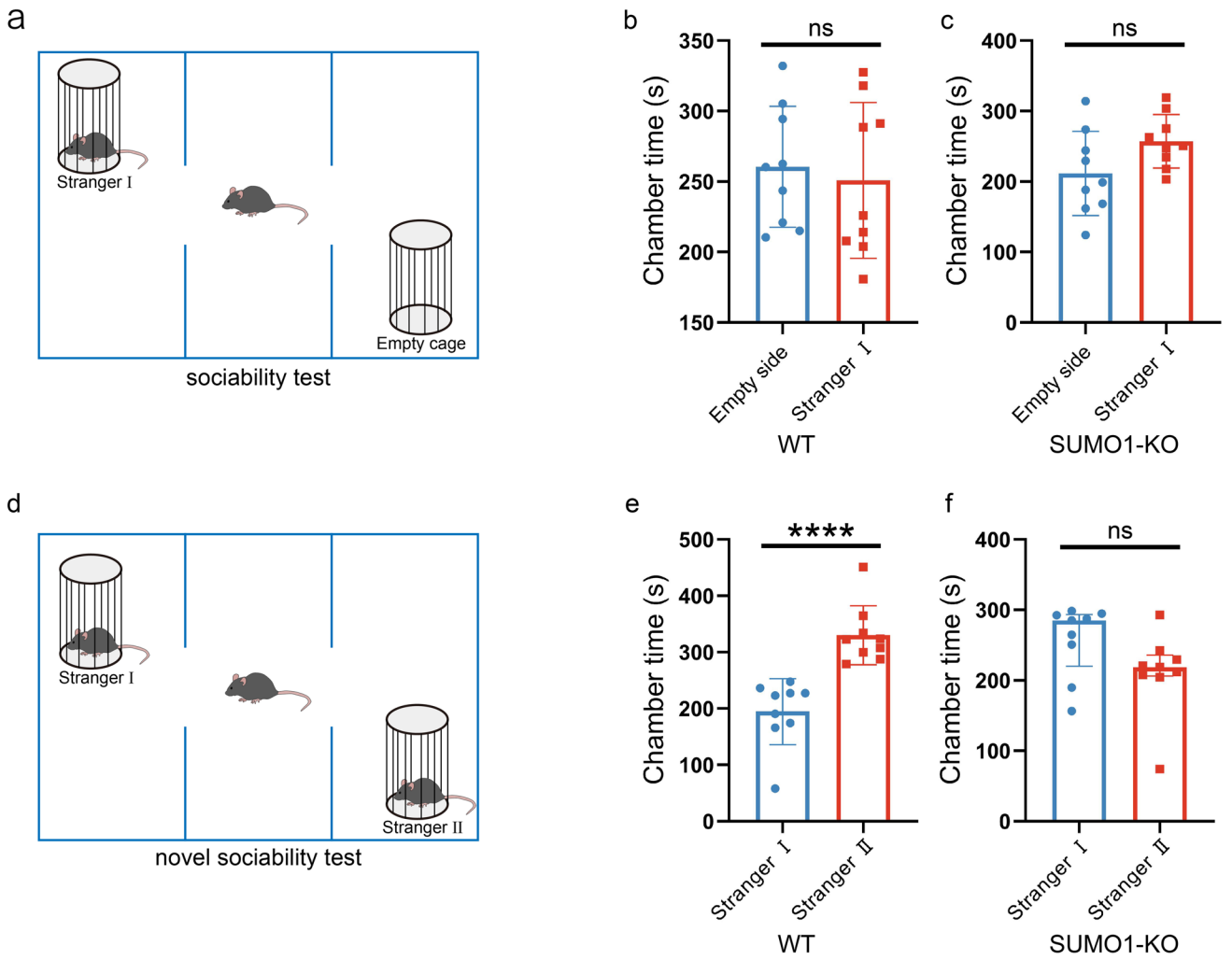

Fig. 3 SUMO1-KO mice exhibit diminished novelty socialization compared to WT controls. **a** Schematic drawing of three-chamber test for sociability test. Created with adobe illustrator. Quantification of social interaction in sociability test for WT mice (**b**) and SUMO1-KO mice (**c**). **d** Schematic drawing of three-chamber test for novel sociability test. Created with adobe illustrator. Quantification of social interaction in novel sociability test for WT mice (**e**) and SUMO1-KO mice (**f**). Data for **f** was represented as median and interquartile range, and the other data were represented as mean ± SD. ****$p < 0.0001$ versus the WT group. $n = 9$ for each group

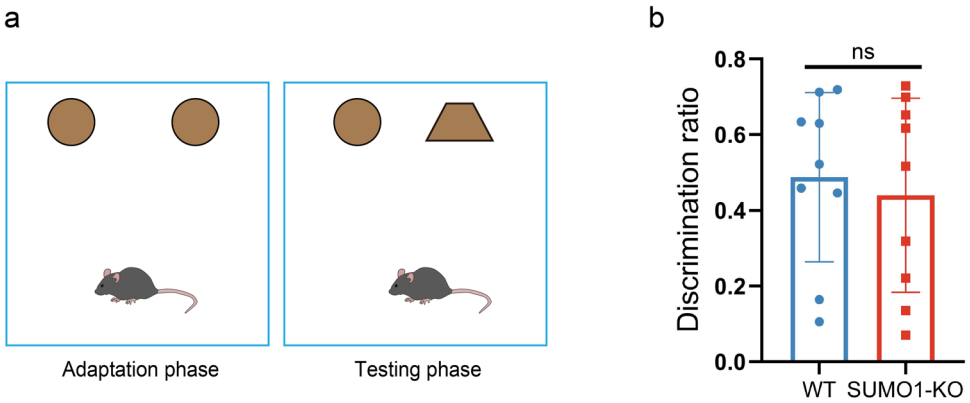

Fig. 4 SUMO1-KO mice displayed comparable memory and cognitive abilities compared to WT controls. **a** Discrimination ratio in the two groups. **b** Recognition index in the two groups. Data are represented as mean ± SD. $n = 9$ for each group

Qualitative and Quantitative Analysis of Proteins

Based on the filtration standard of FDR ≤ 0.01, a total numbers of 136,443 precursors, 116,940 peptides, 8098 protein groups and 8304 proteins were identified (Fig. 5a). For nearly majority of proteins, the number of peptides was greater than or equal to 11 (Fig. 5b). The distribution of quantitative peptide values after normalization was shown

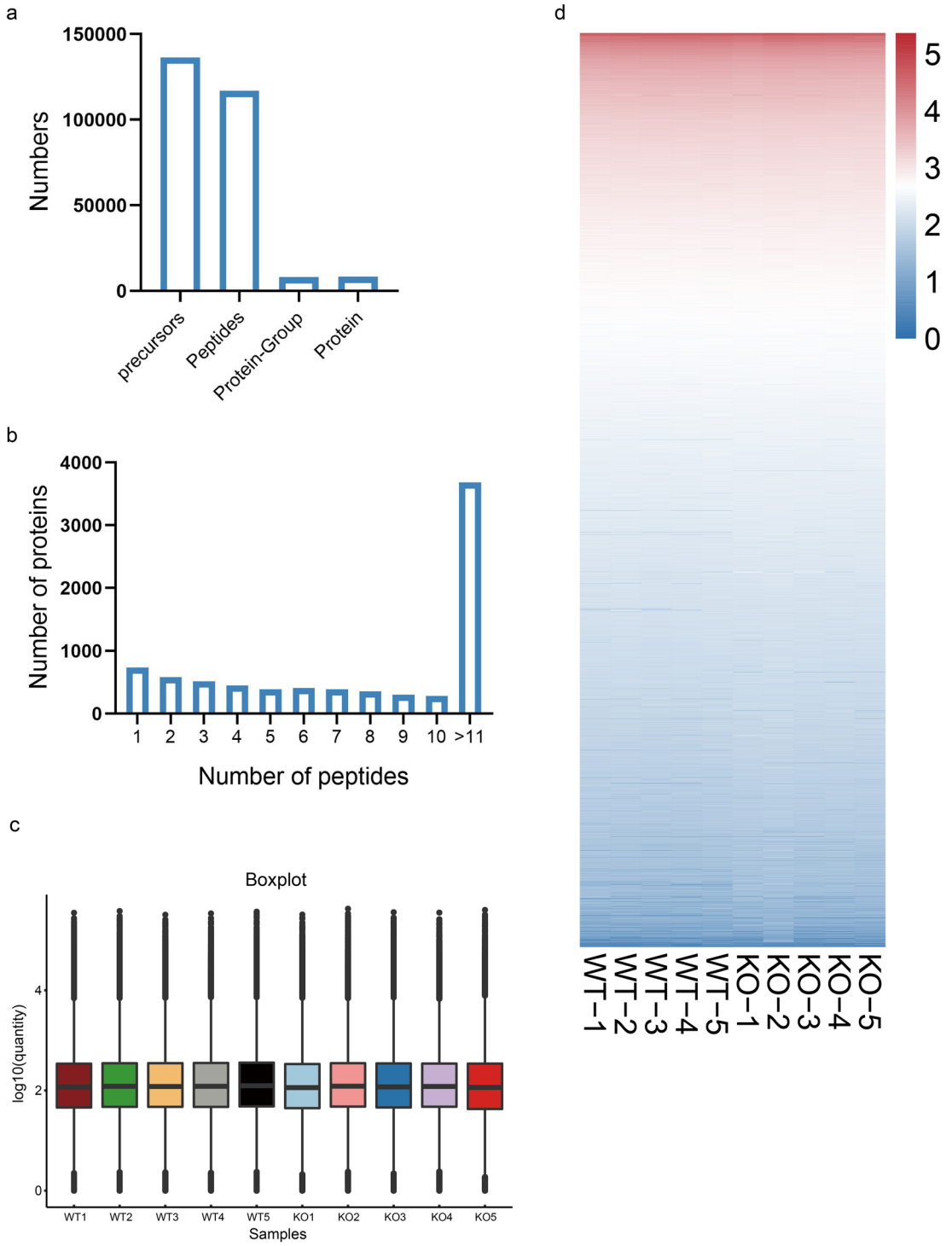

Fig. 5 Qualitative and quantitative analysis of proteins in proteomic of WT group and SUMO1-KO group. **a** The numbers of precursors, peptides, protein groups and proteins that were identified. **b** The distribution of peptide number. **c** The distribution of quantitative peptide values after normalization. **d** The quantitative heatmap of all proteins. $n = 5$ for each group

in Fig. 5c, and the results showed that the signal strength of most samples achieves basically the same response strength. The peak area of peptides with FDR less than 1.0% were selected for protein quantification, and the quantitative heat maps of all proteins are shown in Fig. 5d. Perform log10 calculation on all protein expression levels.

Sample Relationship Analysis

To assess the reproducibility across samples, we calculated the Pearson correlation coefficient based on protein expression levels between each pair of samples. As shown in Fig. 6a, we calculated the Pearson correlation coefficient for each sample pair, and visually represented these correlation coefficients as a heatmap. This heatmap effectively illustrates the degree of correlation between any two samples.

To further evaluate within-group reproducibility, we utilized scatter plots of randomly selected samples from each group. The Pearson correlation between two randomly chosen samples in both the WT and SUMO1-KO groups (Fig. 6b). The results demonstrated a high level of reproducibility within each group.

Differentially Expressed Proteins Analysis

A threshold of absolute FC > 1.2 and p value < 0.05 was applied to identify proteins with significant expression differences between groups. Based on these criteria, 370 proteins were found to be upregulated, and 84 proteins were downregulated in SUMO1-KO group relative to WT group (Fig. 7a). To visualize the differential expression patterns, heatmap was generated where each row represents one protein (Fig. 7b).

Volcano plot (Fig. 7c) and multi-group differential scatter plot (Fig. 7d) were used to provide intuitive overview of the differentially expressed proteins between groups. Red points indicate upregulated proteins in SUMO1-KO group relative to WT group, while blue points represent downregulated proteins. To visually represent the top 20 proteins with the most significant differences between the two sample groups (ranked by p value), one radar chart was created. Each axis on the radar chart corresponds to one of the top 20 differentially expressed proteins, with the central point representing the legend. The outermost values on each axis indicate the values of log2(FC) for these proteins, allowing for an intuitive comparison of expression levels across the WT and SUMO1-KO groups (Fig. 7e).

GO annotation enrichment analysis of differentially expressed proteins indicated that multiple amino acid transmembrane transporter activities including amino transmembrane transporter activity, and multiple ion channel proteins including voltage-gated ion channel activity were significantly enriched (Fig. 7f).

Brain Function-Related Differentially Expressed Proteins Identification

Based on the findings of our behavioral analysis and proteomic differential expression analyses, we conducted a literature review focusing on proteins associated with brain functions. This allowed us to compile a small-scale protein database closely implicated in brain function. Next, an intersection analysis was performed between the differentially expressed proteins identified in this study and the proteins in our protein database to isolate differentially expressed proteins specifically associated with brain function. As a result, six differentially expressed proteins were identified. The finding was presented using Venn diagram to visualize the overlap (Fig. 8a). For the identified brain function-related differentially expressed proteins, one heatmap was

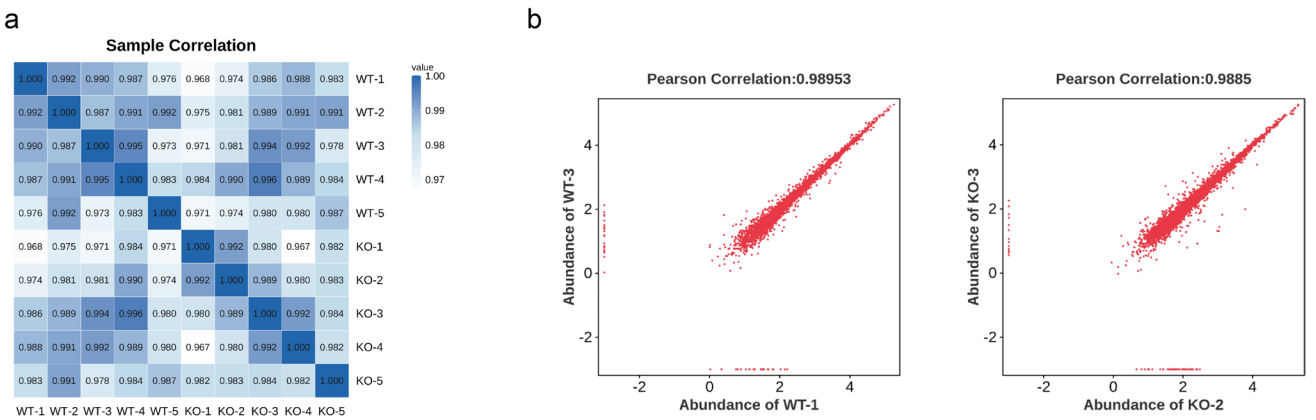

Fig. 6 Sample relationship analysis in proteomic profiling of WT group and SUMO1-KO group. **a** Pearson correlation coefficient heatmap for each sample pair. **b** The Pearson correlation between two randomly chosen samples in both the WT (left) and SUMO1-KO groups (right). $n = 5$ for each group

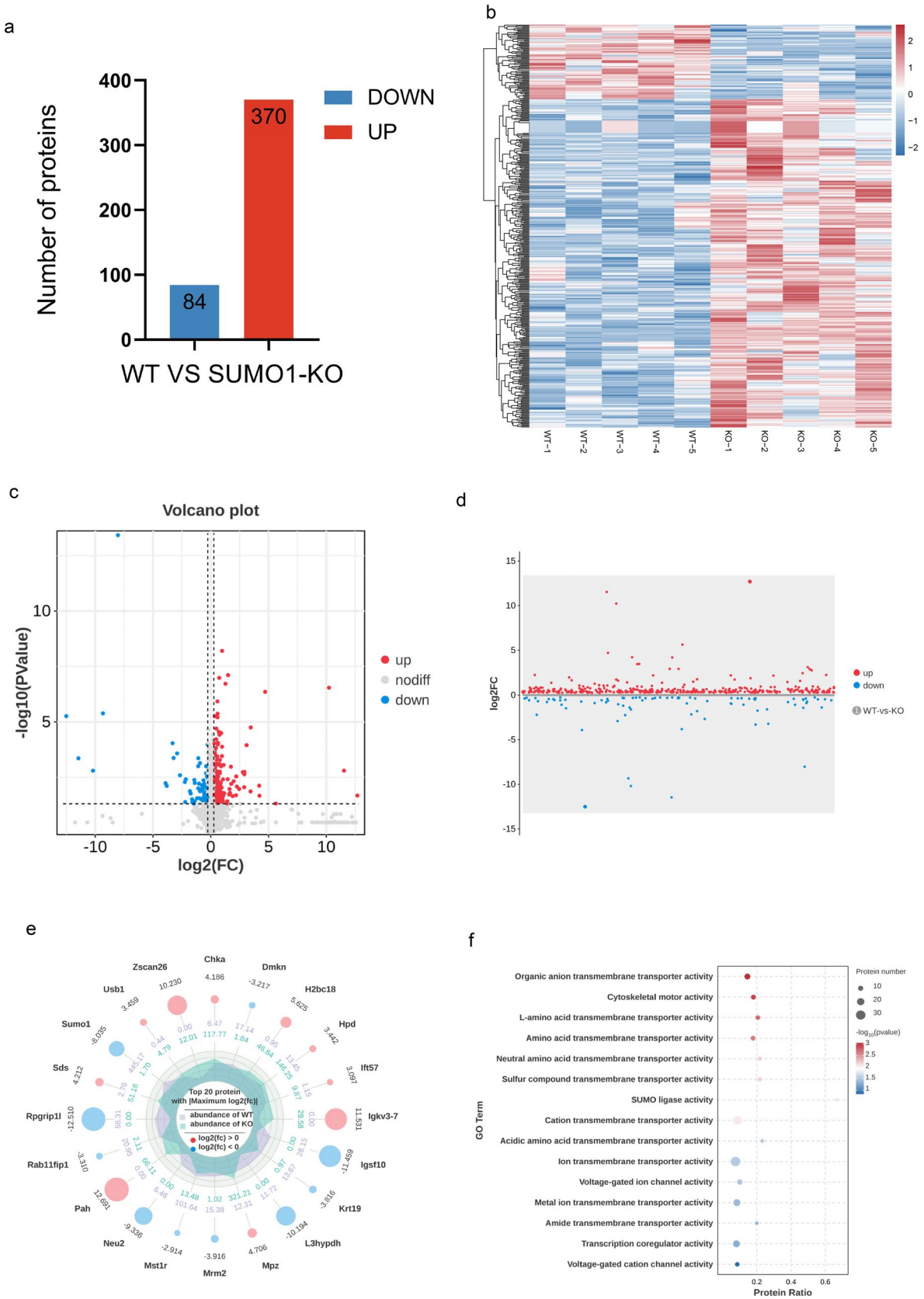
a
Number of proteins
400
300
200
100
0
84
370
DOWN
UP
WT VS SUMO1-KO
b
2
1
0
−1
−2
WT−1
WT−2
WT−3
WT−4
WT−5
KO−1
KO−2
KO−3
KO−4
KO−5
c
Volcano plot
-log10(PValue)
log2(FC)
up
nodiff
down
d
log2FC
up
down
WT-vs-KO
e
Top 20 protein
with |Maximum log2(fc)|
abundance of WT
abundance of KO
log2(fc) > 0
log2(fc) < 0
Zscan26
Chka
Dmkn
Usb1
H2bc18
Sumo1
Hpd
Sds
Ift57
Rpgrip1l
Igkv3-7
Rab11fip1
Igsf10
Pah
Krt19
Neu2
L3hypdh
Mst1r
Mrm2
Mpz
f
Organic anion transmembrane transporter activity
Cytoskeletal motor activity
L-amino acid transmembrane transporter activity
Amino acid transmembrane transporter activity
Neutral amino acid transmembrane transporter activity
Sulfur compound transmembrane transporter activity
SUMO ligase activity
Cation transmembrane transporter activity
Acidic amino acid transmembrane transporter activity
Ion transmembrane transporter activity
Voltage-gated ion channel activity
Metal ion transmembrane transporter activity
Amide transmembrane transporter activity
Transcription coregulator activity
Voltage-gated cation channel activity
GO Term
Protein Ratio
Protein number
-log10(pvalue)

◂**Fig. 7** Differentially expressed proteins analysis in proteomic profiling of WT group and SUMO1-KO group. **a** The number of upregulated and downregulated proteins. **b** Heatmap of differentially expressed proteins. Volcano plot (**c**) and multi-group differential scatter plot (**d**) of the differentially expressed proteins. **e** Radar chart representing the top 20 proteins with the most significant differences. **f** GO annotation analysis of differentially expressed proteins. $n = 5$ for each group

generated to illustrate their expression levels across samples (Fig. 8b). Additionally, the expression levels and log2FC values of the identified brain function-related differentially expressed proteins were shown in Fig. 8c and d, respectively. The results showed that the top two differentially expressed proteins sorted by log2FC value were Rpgrip1l and Hmox1.

SUMO1-KO Mice Exhibit Downregulated Expression Compared to WT Controls of Hmox1 and Rpgrip1l

To validate the downregulated expression of the top two differentially expressed proteins identified by proteomics results, the expression level of Rpgrip1l (Fig. 9a) and Hmox1 (Fig. 9c) in brain tissues of SUMO1-KO and WT group were verified using Western blot. The results showed that the expression level of Hmox1 ($p = 0.0011$, Fig. 9b) and Rpgrip1l ($p = 0.0189$, Fig. 9d) were significantly reduced in SUMO1-KO group compared to WT group, which were consistent with proteomic differential expression analyses. Full western blots showing the marker have been included in the Supplementary Material 3.

Discussion

SUMO1 are involved in the normal physiological functions of the nervous system. As previously reported, SUMO1 is associated with the development of neurodegenerative diseases such as Alzheimer's disease (Nisticò et al. 2014; Hendriks and Vertegaal 2016). Whereas, the effects and underlying mechanisms of SUMO1-KO on emotion- and cognition -related behaviors have not yet been investigated. Our results showed that SUMO1-KO mice exhibit significant yet relatively mild alterations in behavior, including increased risk-taking, reduced depressive symptoms, and diminished novelty socialization compared to WT controls. Furthermore, mass spectrometry-based proteomics analysis identified 370 upregulated and 84 downregulated proteins. GO annotation revealed significant enrichment in processes related to amino acid transmembrane transport and ion channel activity. Further investigation focused on two proteins implicated in behavioral regulation, Hmox1 and Rpgrip1l, both of which were found to be downregulated in the SUMO1-KO mice.

The open filed test is a popular task for evaluating anxiety-like behavior, with mice naturally prefer the outer edges of open field and consider exploring the middle of the field as risky behavior (Pentkowski et al. 2021). Frida A. Lindberg et al. demonstrated that mice deficient in SLC38A10 spent more time in the central zone and visited the central zone more frequently compared to WT mice, suggesting that mice with SLC38A10 deficiency display a greater propensity for exploration and risk-taking (Lindberg et al. 2022). Similarly, our results showed significant increase in central zone distance, central zone distance/total distance and central zone distance/outside zone distance in SUMO1-KO mice (Fig. 1), indicating that SUMO1-KO mice exhibit an increased tendency for exploration and risk-taking behavior relative to WT controls. On the other hand, there were no significant differences between SUMO1-KO mice and WT controls on total distance, activity time, average speed and the number of activities (Fig. 1), suggesting that SUMO1-KO had no significant effects in locomotor ability.

Previous studies have established immobility in tail suspension test as a reliable measure of depressive-like behavior in mice (Cryan et al. 2005). Research conducted by Kavita A. Iyer et al. demonstrated that administration of A7CDQ markedly reduced the immobility times compared to saline treatment, indicating that A7CDQ exerts antidepressant-like effects (Iyer et al. 2019). Additionally, diacylglycerol kinase-η isozyme KO mice showed reduced depressive-like states, as indicated by a decreased immobility time ratio, and this phenotype is similar in behavioral dimensions observed in bipolar disorder during the manic phase (Isozaki et al. 2016). Our result showed that the immobility rate in SUMO1-KO mice was significantly lower than that in WT controls (Fig. 2), suggesting that the SUMO1-KO mice displayed reduced depressive-like behavior, which may reflect a mania-like phenotype.

In the three-chamber test, a comparison between an empty cage and an unfamiliar mouse assesses the social interaction of mice, while a comparison with another unfamiliar mice illustrates the novelty of socialization. Hirotaka Shoji et al. demonstrated that 2-month-old mice spent more time interacting with stranger II than stranger I, whereas no significant difference was observed in the time spent with the two stranger mice in older mice. These observations reflect impaired social recognition in the older mice (Shoji and Miyakawa 2019). In our results, WT mice exhibited significantly longer duration with the stranger II compared to the stranger I, while such trend was not occurred in SUMO1-KO mice (Fig. 3). This finding suggested that SUMO1-KO markedly diminished the novelty socialization. Whereas, there was no significant difference in socialization between SUMO1-KO and WT groups (Fig. 3).

In NOR test, the preference for novel objects is regarded as an indicator of memory and cognitive abilities, often

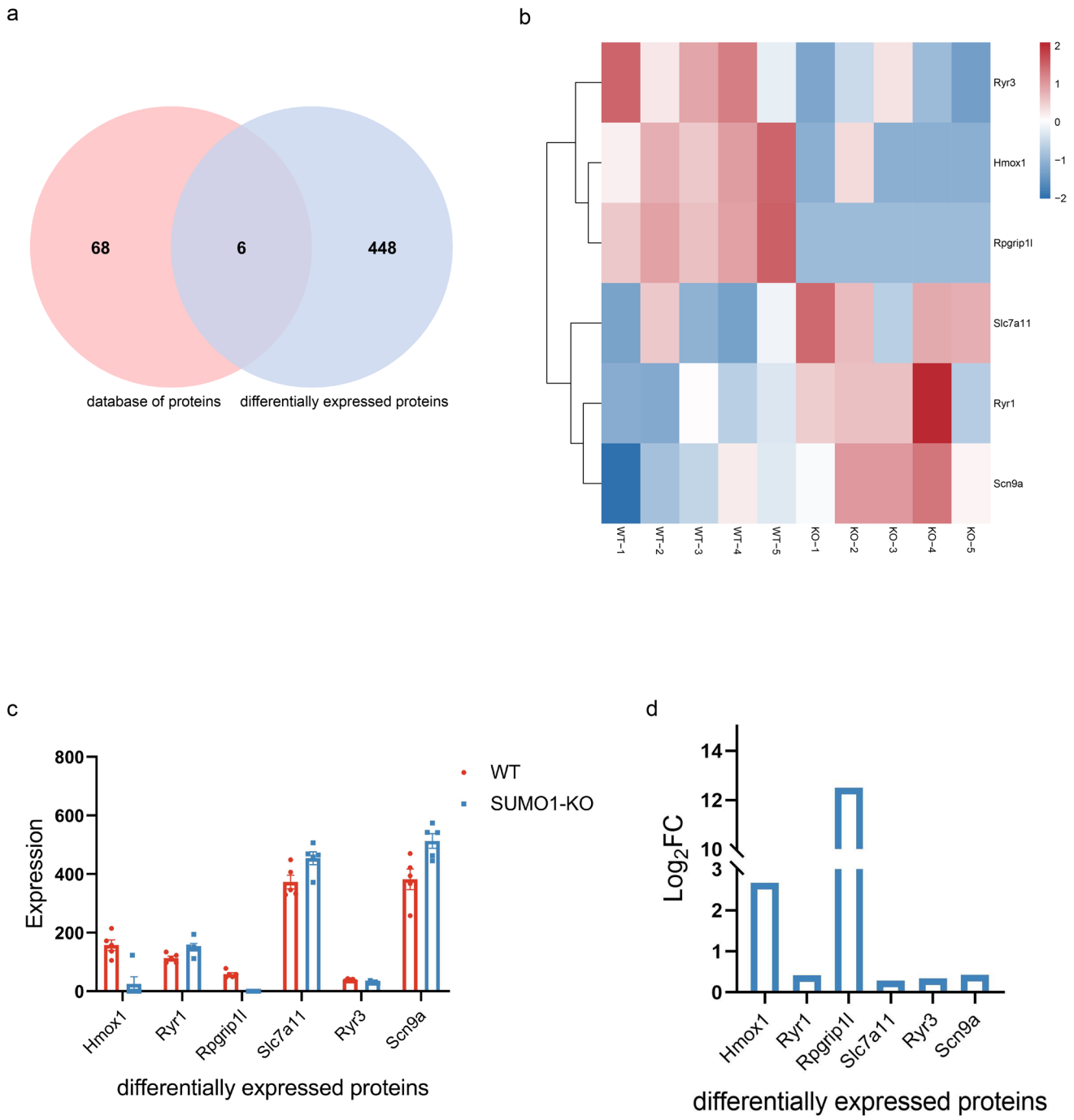

Fig. 8 Brain function-related differentially expressed proteins identification in proteomic profiling of WT group and SUMO1-KO group. **a** Venn diagram to visualize the overlap between the differentially expressed proteins identified in this study and the proteins in our brain function-related protein database. **b** Heatmap of brain function-related differentially expressed proteins. The expression levels (**c**) and log2FC values (**d**) of the identified brain function-related differentially expressed proteins. $n = 5$ for each group

quantified as a recognition index or discrimination rate (Sawangjit et al. 2018; Xu et al. 2019; Shi et al. 2021). Our data showed no significant differences in the discrimination ratio between SUMO1-KO and WT controls (Fig. 4), indicating that memory and cognitive abilities were comparable between SUMO1-KO and WT groups.

To elucidate the behavioral differences between SUMO1-KO and WT mice, we performed proteomic analyses of brain tissues in the two groups. Based on the qualitative and quantitative analysis of proteins analysis (Fig. 5) and sample relationship assessments (Fig. 6), we identified a total of 370 upregulated proteins and 84 downregulated proteins in

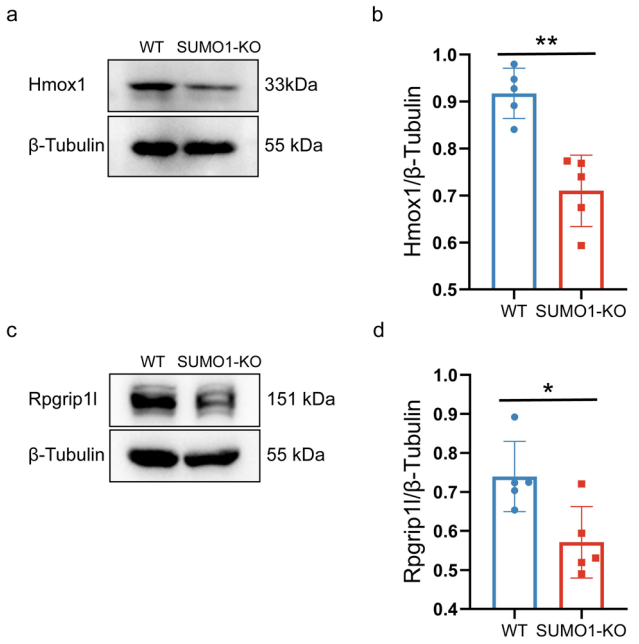

Fig. 9 SUMO1-KO mice exhibit downregulated expression of Hmox1 and Rpgrip1l compared to WT controls. **a** Representative expression of Hmox1 in the two groups. **b** Expression level quantification of Hmox1. **c** Representative expression of Rpgrip1l expressions in the two groups. **d** Expression level quantification of Rpgrip1l. Data are represented as mean ± SD. *$p < 0.05$ versus the WT group. $n = 5$ for each group

SUMO1-KO mice compared to WT controls (Fig. 7). To further ascertain the potential functions of these differentially expressed proteins, GO pathway enrichment analysis was performed.

GO pathway enrichment analysis identified 94 significantly enriched terms, a considerable proportion of which were associated with ion channels and amino acid transporters (Fig. 7). Previous studies have showed that defects in sodium channel, calcium channel and potassium channel were implicated in neurodevelopmental disorders and neurodegenerative disease (Steel et al. 2017; D'Adamo et al. 2020; Kasap and Dwyer 2021; Birey et al. 2022; Haddad et al. 2024). Furthermore, emerging evidence has identified SUMOylation as a relatively novel regulatory mechanism for modulating ion channel function. Specifically, SUMO1 has been shown to silence the dimeric potassium channel K2P1, which plays diverse physiological roles, including apoptosis, neuromodulation, and general anesthesia (Plant et al. 2010). Additionally, SUMOylation of voltage-gated sodium (Na_V) 1.2 channels mediates the early response to acute hypoxia in central neurons, highlighting the SUMO pathway and $Na_V1.2$ as potential targets for neuroprotective interventions (Plant et al. 2016). Moreover, SUMOylation has been reported to activate voltage-gated calcium (Ca_V) 2.2 channels, providing further evidence that $Ca_V2.2$ voltage-gated calcium channels may serve as novel targets within SUMOylation-mediated regulatory pathways (Silveirinha et al. 2021). Glutamate and GABA transporters are vital for maintaining the equilibrium of nervous system function and are critical in the pathogenesis of neurodegenerative, neurological, and dysmorphic neurological disorders (Sears and Hewett 2021). Researches have demonstrated that SUMOylation plays an important role in regulating glutamate homeostasis by modulating both glutamate release from presynaptic terminals (Feligioni et al. 2009) and glutamate uptake (Foran et al. 2014). However, there is currently little research investigating the regulatory mechanisms of SUMO1 in GABA metabolism. Integrating the findings from our GO pathway enrichment analysis with relevant literature suggests that the behavioral alterations observed in SUMO1-KO mice may stem from impaired SUMO1-mediated SUMOylation, leading to dysregulated ion channel function and amino acid metabolism.

By intersecting the aforementioned protein database with differentially expressed proteins identified in this study, six differentially expressed proteins were identified. The top two differentially expressed proteins sorted by log2FC value were Rpgrip1l and Hmox1 (Fig. 8). Consequently, we verified the expression levels of Rpgrip1l and Hmox1 in brain tissues of SUMO1 and WT mice using Western blot, respectively.

Hmox1 catalyzes heme into carbon monoxide, iron, and biliverdin. Disturbances of Hmox1 level was associated with neurodegeneration (Loboda et al. 2016). Overexpression of Hmox1 in neurons has been demonstrated to reduce oxidative damage induced by H_2O_2 and glutamate (Chen et al. 2000). Carbon monoxide, a major product of Hmox1, plays a protective role in both physiological and pathological conditions (Loboda et al. 2015; Ryter and Choi 2016). Additionally, Hmox1 is involved in the neuroinflammatory processes underlying depression (Wang et al. 2024), as well as anxiety (Cheng et al. 2020). Hmox1 overexpression has also been shown to exert beneficial roles in AD and acute ischemic stroke due to its ability of antioxidants, which promote restoration of a suitable redox microenvironment (Si and Wang 2020; Sun et al. 2023). Our results demonstrated a significant reduction in Hmox1 expression in SUMO1-KO mice compared to WT controls (Fig. 9). The decrease in Hmox1 suggested impaired capacity to mitigate oxidative stress, which may contribute to cellular injury, ultimately, abnormal emotional responses in SUMO-1 KO mice.

Rpgrip1l is crucial for the formation of cilia, and primary cilia are essential for central nervous system development. Mouse deficient in Rpgrip1l exhibit neurodevelopmental abnormality (Vierkotten et al. 2007; Andreu-Cervera et al. 2019; Postel et al. 2019; Reissig et al. 2022). Previous studies have also indicated a connection between Rpgrip1l mutations and Joubert syndrome, a ciliopathy characterized by

aberrant brain development and ocular motility disorders (Arts et al. 2007; Delous et al. 2007; Shi et al. 2017). Our results demonstrated a significant reduction in Rpgrip1l expression in SUMO1-KO mice compared to WT controls (Fig. 9). The reduction of Rpgrip1l likely influenced neural development and reduced the production of specific neuronal populations, potentially contributing to abnormal emotional responses in SUMO-1 KO mice.

Conclusion

Based on behavior and underlie proteomic analysis, we concluded that decreased expression of Hmox1 and Rpgrip1l linked to the risk-taking behavior, reduced depressive symptoms, and diminished novelty socialization observed in SUMO1-KO mice. These findings suggested a role for SUMO1 in modulating behavior through regulation of Hmox1 and Rpgrip1l expression, and provided insights into the molecular basis of behavioral changes associated with SUMO1-mediated SUMOylation deficiency.

Limitations

While this study provides novel insights into the behavioral and molecular consequences of SUMO1-KO in aged male mice, several limitations should be acknowledged. First, the relatively small sample sizes in both the proteomics and behavioral experiments may limit the statistical power of our findings. Future studies with larger cohorts are necessary to enhance robustness and ensure the reproducibility of these results. Second, the methodology of western blot could be further optimized to enhance quantification accuracy. Third, in the three-chamber social interaction test, aged WT mice did not exhibit the expected preference for the first social partner (Stranger I) over the empty chamber. This deviation from typical social behavior may be attributed to an age-related decline in social ability; however, further research is needed to elucidate the underlying mechanisms. Forth, this study focused exclusively on male SUMO1-KO mice, leaving the potential sex-dependent effects of SUMO1 deficiency unexplored; Further investigations are required to determine whether SUMO1 knockout induces similar behavioral abnormalities in aged female mice, and explore the underlying molecular mechanisms if such differences exist. Fifth, in addition to the tail suspension test used in this study, incorporating the sucrose preference test and the sucrose splash test would allow for a more comprehensive and precise evaluation of depressive-like behaviors in mice. Finally, further research is needed to explore the role of specific brain regions in the observed behavioral abnormalities in SUMO1-KO mice and the underlying mechanisms. Addressing these limitations in future research will be crucial for developing a more comprehensive understanding of the role of SUMO1 in neurodevelopment, aging, and behavior.

Supplementary Information The online version contains supplementary material available at https://doi.org/10.1007/s10571-025-01548-y.

Acknowledgements The authors gratefully acknowledge Wei Yang, PhD (Duke University Medical Center, USA) for providing SUMO1$^{-/-}$mice.

Author Contributions Conceptualization: Zhiqing Li, Yuxiang Wang, Xiaozhi Liu; Methodology: Qiwei Dai, Yuxiang Wang, Hongbin Xu, He Dong, Fang Nie; Formal analysis and investigation: Qiwei Dai, Yuxiang Wang, Hongbin Xu, He Dong, Fang Nie, Lianxue Zhang; Writing—original draft preparation: Qiwei Dai, Yuxiang Wang, Hongbin Xu; Writing—review and editing: Zhiqing Li; Funding acquisition: Zhiqing Li, Yuxiang Wang, Xiaozhi Liu; Resources: Zhiqing Li, Xiaozhi Liu; Supervision: Zhiqing Li.

Funding This study was supported by Noncommunicable Chronic Diseases-National Science and Technology Major Project (No. 2023ZD0505600), Shenyang Science and Technology Bureau (No. 21–172-9–17), National Clinical Key Specialty Construction Project of the Emergency Department (No. 2023283), Tianjin Municipal Science and Technology Plan Project (No. 24ZYCGSY00650), Tianjin Health Technology Project (No. TJWJ2022XK043), Tianjin Binhai New Area Health Commission Science and Technology Project (No. 2023BWKQ001), Tianjin Municipal Health Commission Scientific Research Project of Traditional Chinese Medicine and Integrated Chinese-Western Medicine (No. 2023187).

Data Availability The proteomics data has been uploaded in iProX, and the ID is PXD059745.

Declarations

Competing interest The authors declare no competing interests.

References

Andreu-Cervera A, Anselme I, Karam A, Laclef C, Catala M, Schneider-Maunoury S (2019) The ciliopathy gene ftm/rpgrip1l controls mouse forebrain patterning via region-specific modulation of Hedgehog/Gli signaling. J Neurosci 39:2398–2415

Arioli M, Cattaneo Z, Rusconi ML, Blandini F, Tettamanti M (2022) Action and emotion perception in Parkinson's disease: a neuroimaging meta-analysis. NeuroImage Clin 35:103031

Arts HH, Doherty D, van Beersum SE, Parisi MA, Letteboer SJ, Gorden NT, Peters TA, Märker T, Voesenek K, Kartono A, Ozyurek H, Farin FM, Kroes HY, Wolfrum U, Brunner HG, Cremers FP, Glass IA, Knoers NV, Roepman R (2007) Mutations in the gene encoding the basal body protein RPGRIP1L, a nephrocystin-4 interactor, cause Joubert syndrome. Nat Genet 39:882–888

Bai B et al (2020) Deep multilayer brain proteomics identifies molecular networks in Alzheimer's disease progression. Neuron 105:975-991.e977

Birey F, Li MY, Gordon A, Thete MV, Valencia AM, Revah O, Paşca AM, Geschwind DH, Paşca SP (2022) Dissecting the molecular basis of human interneuron migration in forebrain assembloids from Timothy syndrome. Cell Stem Cell 29:248-264.e247

Chen K, Gunter K, Maines MD (2000) Neurons overexpressing heme oxygenase-1 resist oxidative stress-mediated cell death. J Neurochem 75:304–313

Cheng J, Li F, Sun X, Liu S, Chen L, Tian F, Zhao Z, Hu H, Li X (2020) Low-dose alcohol ameliorated homocysteine-induced anxiety-related behavior via attenuating oxidative stress in mice. Neurosci Lett 714:134568

Cryan JF, Mombereau C, Vassout A (2005) The tail suspension test as a model for assessing antidepressant activity: review of pharmacological and genetic studies in mice. Neurosci Biobehav Rev 29:571–625

D'Adamo MC, Liantonio A, Conte E, Pessia M, Imbrici P (2020) Ion channels involvement in neurodevelopmental disorders. Neuroscience 440:337–359

Delous M et al (2007) The ciliary gene RPGRIP1L is mutated in cerebello-oculo-renal syndrome (Joubert syndrome type B) and Meckel syndrome. Nat Genet 39:875–881

Evdokimov E, Sharma P, Lockett SJ, Lualdi M, Kuehn MR (2008) Loss of SUMO1 in mice affects RanGAP1 localization and formation of PML nuclear bodies, but is not lethal as it can be compensated by SUMO2 or SUMO3. J Cell Sci 121:4106–4113

Feligioni M, Nishimune A, Henley JM (2009) Protein SUMOylation modulates calcium influx and glutamate release from presynaptic terminals. Eur J Neurosci 29:1348–1356

Foran E, Rosenblum L, Bogush A, Pasinelli P, Trotti D (2014) Sumoylation of the astroglial glutamate transporter EAAT2 governs its intracellular compartmentalization. Glia 62:1241–1253

Gonzales MM, Garbarino VR, Pollet E, Palavicini JP, Kellogg DL, Jr., Kraig E, Orr ME (2022) Biological aging processes underlying cognitive decline and neurodegenerative disease. J Clin Investig 132

Haddad S, Ablinger C, Stanika R, Hessenberger M, Campiglio M, Ortner NJ, Tuluc P, Obermair GJ (2025) A biallelic mutation in CACNA2D2 associated with developmental and epileptic encephalopathy affects calcium channel-dependent as well as synaptic functions of α(2)δ-2. J Neurochem 169:e16197

Hay RT (2005) SUMO: a history of modification. Mol Cell 18:1–12

Hendriks IA, Vertegaal AC (2016) A comprehensive compilation of SUMO proteomics. Nat Rev Mol Cell Biol 17:581–595

Hou Y, Dan X, Babbar M, Wei Y, Hasselbalch SG, Croteau DL, Bohr VA (2019) Ageing as a risk factor for neurodegenerative disease. Nat Rev Neurol 15:565–581

Isozaki T, Komenoi S, Lu Q, Usuki T, Tomokata S, Matsutomo D, Sakai H, Bando K, Kiyonari H, Sakane F (2016) Deficiency of diacylglycerol kinase η induces lithium-sensitive mania-like behavior. J Neurochem 138:448–456

Iyer KA, Alix K, Eltit JM, Solis E Jr, Pan X, Argade MD, Khatri S, De Felice LJ, Sweet DH, Schulte MK, Dukat M (2019) Multi-modal antidepressant-like action of 6- and 7-chloro-2-aminodihydroquinazolines in the mouse tail suspension test. Psychopharmacology 236:2093–2104

Jackson SP, Durocher D (2013) Regulation of DNA damage responses by ubiquitin and SUMO. Mol Cell 49:795–807

Karayel O, Virreira Winter S, Padmanabhan S, Kuras YI, Vu DT, Tuncali I, Merchant K, Wills AM, Scherzer CR, Mann M (2022) Proteome profiling of cerebrospinal fluid reveals biomarker candidates for Parkinson's disease. Cell Rep Med 3:100661

Kasap M, Dwyer DS (2021) Na(+) leak-current channel (NALCN) at the junction of motor and neuropsychiatric symptoms in Parkinson's disease. J Neural Transm 128:749–762

Krumova P, Weishaupt JH (2013) Sumoylation in neurodegenerative diseases. Cell Mol Life Sci: CMLS 70:2123–2138

Lee L, Sakurai M, Matsuzaki S, Arancio O, Fraser P (2013) SUMO and Alzheimer's disease. NeuroMol Med 15:720–736

Lindberg FA, Nordenankar K, Fredriksson R (2022) SLC38A10 knockout mice display a decreased body weight and an increased risk-taking behavior in the open field test. Front Behav Neurosci 16:840987

Liu Q, Xi Y, Wang Q, Liu J, Li P, Meng X, Liu K, Chen W, Liu X, Liu Z (2021) Mannan oligosaccharide attenuates cognitive and behavioral disorders in the 5xFAD Alzheimer's disease mouse model via regulating the gut microbiota-brain axis. Brain Behav Immun 95:330–343

Loboda A, Jozkowicz A, Dulak J (2015) HO-1/CO system in tumor growth, angiogenesis and metabolism—targeting HO-1 as an anti-tumor therapy. Vascul Pharmacol 74:11–22

Loboda A, Damulewicz M, Pyza E, Jozkowicz A, Dulak J (2016) Role of Nrf2/HO-1 system in development, oxidative stress response and diseases: an evolutionarily conserved mechanism. Cell Mol Life Sci 73:3221–3247

Lomelí H, Vázquez M (2011) Emerging roles of the SUMO pathway in development. Cell Mol Life Sci 68:4045–4064

Nisticò R, Ferraina C, Marconi V, Blandini F, Negri L, Egebjerg J, Feligioni M (2014) Age-related changes of protein SUMOylation balance in the AβPP Tg2576 mouse model of Alzheimer's disease. Front Pharmacol 5:63

Pentkowski NS, Rogge-Obando KK, Donaldson TN, Bouquin SJ, Clark BJ (2021) Anxiety and Alzheimer's disease: Behavioral analysis and neural basis in rodent models of Alzheimer's-related neuropathology. Neurosci Biobehav Rev 127:647–658

Plant LD, Dementieva IS, Kollewe A, Olikara S, Marks JD, Goldstein SA (2010) One SUMO is sufficient to silence the dimeric potassium channel K2P1. Proc Natl Acad Sci USA 107:10743–10748

Plant LD, Marks JD, Goldstein SA (2016) SUMOylation of Na(V)1.2 channels mediates the early response to acute hypoxia in central neurons. eLife 5

Postel M, Karam A, Pézeron G, Schneider-Maunoury S, Clément F (2019) A multiscale mathematical model of cell dynamics during neurogenesis in the mouse cerebral cortex. BMC Bioinform 20:470

Reissig LF, Geyer SH, Winkler V, Preineder E, Prin F, Wilson R, Galli A, Tudor C, White JK, Mohun TJ, Weninger WJ (2022) Detailed characterizations of cranial nerve anatomy in E14.5 mouse embryos/fetuses and their use as reference for diagnosing subtle, but potentially lethal malformations in mutants. Front Cell Dev Biol 10:1006620

Rose MR (2009) Adaptation, aging, and genomic information. Aging 1:444–450

Ryter SW, Choi AM (2016) Targeting heme oxygenase-1 and carbon monoxide for therapeutic modulation of inflammation. Transl Res: J Lab Clin Med 167:7–34

Sawangjit A, Oyanedel CN, Niethard N, Salazar C, Born J, Inostroza M (2018) The hippocampus is crucial for forming non-hippocampal long-term memory during sleep. Nature 564:109–113

Sears SM, Hewett SJ (2021) Influence of glutamate and GABA transport on brain excitatory/inhibitory balance. Exp Biol Med 246:1069–1083

Shi X, Garcia G 3rd, Van De Weghe JC, McGorty R, Pazour GJ, Doherty D, Huang B, Reiter JF (2017) Super-resolution microscopy reveals that disruption of ciliary transition-zone architecture causes Joubert syndrome. Nat Cell Biol 19:1178–1188

Shi X, Bai H, Wang J, Wang J, Huang L, He M, Zheng X, Duan Z, Chen D, Zhang J, Chen X, Wang J (2021) Behavioral assessment of sensory, motor, emotion, and cognition in rodent models of intracerebral hemorrhage. Front Neurol 12:667511

Shoji H, Miyakawa T (2019) Age-related behavioral changes from young to old age in male mice of a C57BL/6J strain maintained under a genetic stability program. Neuropsychopharmacol Rep 39:100–118

Si Z, Wang X (2020) The neuroprotective and neurodegeneration effects of heme oxygenase-1 in Alzheimer's disease. J Alzheimer's Dis 78:1259–1272

Silveirinha V, Stephens GJ, Cimarosti H (2013) Molecular targets underlying SUMO-mediated neuroprotection in brain ischemia. J Neurochem 127:580–591

Silveirinha VC, Lin H, Tanifuji S, Mochida S, Cottrell GS, Cimarosti H, Stephens GJ (2021) Ca(V)2.2 (N-type) voltage-gated calcium channels are activated by SUMOylation pathways. Cell Calcium 93:102326

Steel D, Symonds JD, Zuberi SM, Brunklaus A (2017) Dravet syndrome and its mimics: beyond SCN1A. Epilepsia 58:1807–1816

Sun YY, Zhu HJ, Zhao RY, Zhou SY, Wang MQ, Yang Y, Guo ZN (2023) Remote ischemic conditioning attenuates oxidative stress and inflammation via the Nrf2/HO-1 pathway in MCAO mice. Redox Biol 66:102852

Takano T, Wallace JT, Baldwin KT, Purkey AM, Uezu A, Courtland JL, Soderblom EJ, Shimogori T, Maness PF, Eroglu C, Soderling SH (2020) Chemico-genetic discovery of astrocytic control of inhibition in vivo. Nature 588:296–302

Tang JJ, Huang LF, Deng JL, Wang YM, Guo C, Peng XN, Liu Z, Gao JM (2022) Cognitive enhancement and neuroprotective effects of OABL, a sesquiterpene lactone in 5xFAD Alzheimer's disease mice model. Redox Biol 50:102229

Vierkotten J, Dildrop R, Peters T, Wang B, Rüther U (2007) Ftm is a novel basal body protein of cilia involved in Shh signalling. Development 134:2569–2577

Wang J, Behl T, Rana T, Sehgal A, Wal P, Saxena B, Yadav S, Mohan S, Anwer MK, Chigurupati S, Zaheer I, Shen B, Singla RK (2024) Exploring the pathophysiological influence of heme oxygenase-1 on neuroinflammation and depression: A study of phytotherapeutic-based modulation. Phytomed: Int J Phytother Phytopharmacol 127:155466

Xie W, Guo D, Li J, Yue L, Kang Q, Chen G, Zhou T, Wang H, Zhuang K, Leng L, Li H, Chen Z, Gao W, Zhang J (2022) CEND1 deficiency induces mitochondrial dysfunction and cognitive impairment in Alzheimer's disease. Cell Death Differ 29:2417–2428

Xu XE, Liu L, Wang YC, Wang CT, Zheng Q, Liu QX, Li ZF, Bai XJ, Liu XH (2019) Caspase-1 inhibitor exerts brain-protective effects against sepsis-associated encephalopathy and cognitive impairments in a mouse model of sepsis. Brain Behav Immun 80:859–870

Yang W, Sheng H, Thompson JW, Zhao S, Wang L, Miao P, Liu X, Moseley MA, Paschen W (2014) Small ubiquitin-like modifier 3-modified proteome regulated by brain ischemia in novel small ubiquitin-like modifier transgenic mice: putative protective proteins/pathways. Stroke 45:1115–1122

Zhang Z, Wu S, Stenoien DL, Paša-Tolić L (2014) High-throughput proteomics. Annu Rev Anal Chem 7:427–454

Authors and Affiliations

Qiwei Dai[1] · Yuxiang Wang[2] · Hongbin Xu[3] · He Dong[1] · Fang Nie[1] · Lianxue Zhang[1] · Xiaozhi Liu[2,4,5] · Zhiqing Li[1,3,6]

✉ Zhiqing Li
dr_lizhiqing@163.com; lizq@cmu.edu.cn

[1] Department of Stroke Center, The First Hospital of China Medical University, Shenyang 110001, Liaoning, People's Republic of China

[2] Central Laboratory, Tianjin Key Laboratory of Epigenetic for Organ Development of Preterm Infants, Tianjin Fifth Central Hospital, Tianjin 300450, People's Republic of China

[3] Department of Neurosurgery, The First Hospital of China Medical University, Shenyang 110001, Liaoning, People's Republic of China

[4] The Emergency Center, Tianjin Fifth Central Hospital, Tianjin 300450, People's Republic of China

[5] Tianjin Binhai Huangnan Plateau Medical Research Institute, Huangnan Tibetan Autonomous Prefecture People's Hospital, Huangnan Prefecture 811399, Qinghai Province, People's Republic of China

[6] Department of Neurology, The First Hospital of China Medical University, Shenyang 110001, Liaoning, People's Republic of China